Facile synthesis of $NiCo_2O_4$@Polyaniline CORE-shell nanocomposite for sensitive determination of glucose

Zhiyuan Yu, Hejun Li, Xinmeng Zhang, Ningkun Liu, Wenlong Tan, Xu Zhang, Leilei Zhang

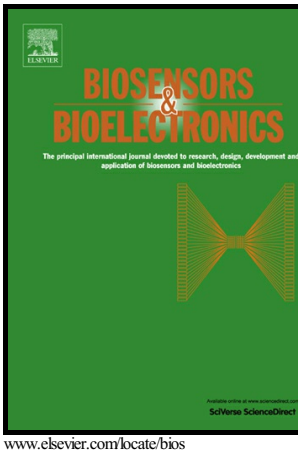

www.elsevier.com/locate/bios

PII: S0956-5663(15)30350-X
DOI: http://dx.doi.org/10.1016/j.bios.2015.08.024
Reference: BIOS7920

To appear in: *Biosensors and Bioelectronic*

Received date: 29 June 2015
Revised date: 12 August 2015
Accepted date: 14 August 2015

Cite this article as: Zhiyuan Yu, Hejun Li, Xinmeng Zhang, Ningkun Liu Wenlong Tan, Xu Zhang and Leilei Zhang, Facile synthesis o $NiCo_2O_4$@Polyaniline CORE-shell nanocomposite for sensitive determination o glucose, *Biosensors and Bioelectronic* http://dx.doi.org/10.1016/j.bios.2015.08.024

Facile synthesis of $NiCo_2O_4$@Polyaniline core-shell nanocomposite for sensitive determination of glucose

Zhiyuan Yu, Hejun Li*, Xinmeng Zhang, Ningkun Liu, Wenlong Tan, Xu Zhang, Leilei Zhang

State Key Laboratory of Solidification Processing, Carbon/Carbon Composites Research Center, Northwestern Polytechnical University, Xi'an 710072, China

Corresponding authors *Hejun Li, E-mail address: lihejun@nwpu.edu.cn

ABSTRACT: In this work, the core-shell structure of $NiCo_2O_4$@Polyaniline ($NiCo_2O_4$@PANI) nanocomposite is fabricated via a facile hydrothermal treatment followed by a post Polyaniline (PANI) coating process. The synthesized materials are characterized by Transmission electron microscopy (TEM), X-ray diffraction (XRD), X-ray photoelectron spectroscopy (XPS) and Raman spectrometer. The biosensing properties of $NiCo_2O_4$@PANI composite and $NiCo_2O_4$ nanoparticles toward glucose are studied based on glassy carbon electrode. Electrochemical studies indicate that the obtained core-shell $NiCo_2O_4$@PANI composite shows higher electrocatalytic activity toward the oxidation of glucose, compared with $NiCo_2O_4$ nanoparticles. The enhanced performance is related to the core-shell structure of $NiCo_2O_4$@PANI composite and the outstanding conductivity of the polyaniline shell. At a potential of +0.5 V, the $NiCo_2O_4$@PANI nanocomposite modified glass carbon electrode demonstrates a wide linear range up to 4.7350 mM with sensitivity of 4.55 mA mM^{-1} cm^{-2} and detection limit of 0.3833 μM. It also shows significant electrochemical stability, good reproducibility and excellent selectivity. The results suggest that the $NiCo_2O_4$@PANI

nanocomposite is a promising electrode material for electrochemical biosensor.

Keywords: $NiCo_2O_4$, Polyaniline, core-shell, Glucose sensor

1. Introduction

The measurement of glucose is important for the diagnosis and control of diabetes (Kotanen et al., 2012). Early glucose biosensor is analyzed with enzymatic reactions suffering from draw backs such as complicated immobilization techniques, rigorous operating conditions, and inherent instability (Yoo and Lee, 2010; Wang et al., 2008; Zhang et al.,2015). Thus, it is of great importance to develop a sensitive and selective non-enzymatic sensor for the determination of glucose.

Up to now, several possible metal oxides and complex metal oxides, such as NiO (El-Refaei and Saleh, 2013; Cao et al., 2011), Co_3O_4 (Li et al., 2015), CuO (Sun et al, 2013; Yang et al., 2011), ZnO (Pradhan et al., 2010), MnO_2 (Ye et al., 2013), and $NiCo_2O_4$ (Yu et al., 2014), have been explored for sensor applications. Among them, $NiCo_2O_4$ nanostructures are one of the promising mixed-metal oxides for biosensors due to its electrochemical catalytic activity, biocompatibility, and nontoxicity. Recent studies have demonstrated that $NiCo_2O_4$ has much better electronic conductivity, at least 2 orders of magnitude higher than that of either nickel oxide or cobalt oxide (Hu et al., 2012). Moreover, the incorporation of Ni atoms into Co_3O_4 results in $NiCo_2O_4$, which provides more catalytically active sites and simultaneously offers numerous effective electrolyte-accessible channels for ion transportation. However, the poor intrinsic electronic conductivity of $NiCo_2O_4$ still hinders the electron transportation

and decelerates redox reactions, which always results in low sensitivity and stability. Constructing a core-shell structure, particularly the conductive substrates coating as the outer walls of mental oxides, is one of the most important strategies for improving their conductivities (Zhao et al., 2012; Jeong et al., 2013; Li et al., 2015). Among all conductive nanostructured substrates, polyaniline based composite materials have attracted much attention owing to its high electrical conductivity, ease of preparation and good environmental stability (Jeong et al., 2013; Wang et al., 2014; Xu et al., 2014; Gumpu et al., 2014). However, the current research for PANI-based composite materials mainly focuses on the simple individual metal oxides. The investigation on fabrication of complex metal oxides/PANI core-shell composites and their biosensor performances exploration has been rarely reported. And it is still a challenging task to develop a simple and reliable strategy for constructing the core-shell arrays of metal oxide and PANI with a controlled size, and morphology under mass manufacture.

In this study, we develop a simple approach for the fabrication of core-shell structures of $NiCo_2O_4$@PANI using a facile hydrothermal treatment followed by in situ polymerization coating process. Through coating shell PANI, the $NiCo_2O_4$@PANI core-shell structure can combine the merits of good contact and efficient diffusion distances for electron transports, which leads to fast reaction kinetics. The results indicate that the as-prepared composite exhibits excellent sensor performances such as wide linear range, high sensitivity, low detection limit and good selectivity. Moreover, due to the good protection of PANI shell, the core-shell composite shows significant electrochemical stability. Therefore, the $NiCo_2O_4$@PANI

composite can be a promising candidate for the biosensor material.

2. Experimental

2.1. Preparation of $NiCo_2O_4$ nanoparticles.

All the reagents used in the experiment were of analytical grade and were used without further purification. First, $NiCl_2 \cdot 6H_2O$ (2.38 g, Sigma-Aldrich), $CoCl_2 \cdot 6H_2O$ (4.74 g, Sigma-Aldrich) and polyvinyl pyrrolidone (PVP, 1.0 g) were dispersed in water (200 mL) and N-methyl-2-pyrrolidone (NMP, 50 mL) with sonication for 0.5h. Then the obtained solution was sealed into Teflon-lined stainless-steel autoclave for hydrothermal reaction at 200 °C for 4 hours. After that, the resulting sample was cooled to room temperature (RT). Finally, the products were filtered and washed several times with water and ethanol.

2.2. Preparation of $NiCo_2O_4$@PANI composite.

The above prepared $NiCo_2O_4$ powder (0.46 g) was dispersed in NMP solution (30 mL). An aniline monomer solution (0.1 g) was added and the mixture was stirred at RT for 12 hours. The resulting mixture was washed by NMP to remove the unbound aniline monomers. The obtained solution was dispersed in NMP solution, followed by the addition of ammonium persulfate (0.2 g) and HCl (0.1 mL) solution. Subsequently, the mixture was placed on a magnetic stirrer at 0 °C for 2 h. The final products were collected by filtration, and washed several times with ethanol.

2.3. Characterization.

The morphologies and structures of the materials were characterized by X-ray diffraction (XRD, X'Pert Pro MPD), X-ray photoelectron spectroscopy (XPS,

PHI-5400), Transmission electron microscopy (TEM, Tecnai F30 G^2) and Raman spectrometer (Renishaw, United Kingdom).

2.4. Electrochemical Testing.

The electrochemical measurements were carried out in a three electrode electrochemical cell on a CS310 electrochemical workstation (Corrtest, China). The $NiCo_2O_4$@PANI composite modified glassy carbon (GC) electrode was used as the working electrode. Ag/AgCl electrode and platinum plate were used as the reference and counter electrode. The GC electrode was polished with alumina powder and cleaned by sonication before the deposition of $NiCo_2O_4$@PANI onto the electrode surface. Then a required amount of samples was ultrasonically dispersed in 0.081% Nafion solution to achieve a 0.5 mg/mL uniform ink. Finally, 10 μL of the ink was dropped on the GC electrode and dried before the electrochemical experiments.

3. Results and discussion

3.1. Characterization of $NiCo_2O_4$@PANI composite.

The structure and morphology of the $NiCo_2O_4$@PANI core-shell composite is confirmed by the high-resolution transmission electron microscopy (HRTEM). As can be seen in Figure 1a, the average diameters of these $NiCo_2O_4$@PANI nanoparticles are only about 25 nm greatly shortening ion-transport pathways. Moreover, the HRTEM images in Figure 1b and c further confirm the core-shell structure of $NiCo_2O_4$@PANI. It can be seen that the $NiCo_2O_4$ nanoparticles are highly crystalline with distinct lattice fringes and the thickness of the PANI shell ranges from several nanometers to tens of nanometers. The PANI shell structure can combine the merits of

good contact and efficient diffusion distances for electron transports, which enhances the sensor property (Zhai et al., 2013). Additionally, the energy dispersive X-ray spectroscopy (EDS) pattern is also conducted from the square area of the $NiCo_2O_4$@PANI core-shell composite (Figure 1d), confirming the existence of elements such as Ni, Co, O, Cl, C and N. The elements C and N prove the existence of the PANI. Besides, the element Cl may come from the interface of the core-shell structure, which is wrapped up by PANI. The composition analysis demonstrates the stoichiometry Ni : Co : O in the sample is about 1 : 2 : 4, which certifies the successful preparation of $NiCo_2O_4$.

Figure 1 here

Figure S1 shows the XRD patterns of as-prepared products. The XRD pattern can be indexed to the (111), (220), (311), (400), (511), (440), and (533) reflections of face-centered cubic-structured $NiCo_2O_4$ (JCPDS 73-1702). However, compared with $NiCo_2O_4$, the $NiCo_2O_4$@PANI composite exhibits no obvious additional peak of crystalline. The result reveals that the $NiCo_2O_4$ particle hinders the PANI molecular chains organization, which demonstrates the PANI shell is amorphous (Wang et al., 2014; Xia and Wang, 2002).

XPS technique is used to investigate the chemical state of the as-prepared $NiCo_2O_4$@PANI composite in our study. As shown in Figure S2, the survey spectrum indicates the presence of Ni, Co, O, C and N element from $NiCo_2O_4$@PANI. Using a

Gaussian fitting method, the Ni 2p spectrum could also be fitted into two spin–orbit doublets, characteristics of Ni^{2+} and Ni^{3+}, and two shakeup satellites. The fitting peaks at 854.28 and 871.28 eV are indexed to Ni^{2+}, while the other fitting peaks at 856.08 and 873.58 eV are ascribed to Ni^{3+}. Similarly, In Co 2p spectra, two kinds of Co species are observed and assigned to the species containing Co^{2+} and Co^{3+}. The fitting peaks at 780.98 and 795.68 eV are attributed to Co^{2+}, while the other two fitting peaks at 779.88 and 794.68 eV belong to Co^{3+}. All these facts reveal that the chemical composition of as-prepared $NiCo_2O_4$ contains Ni^{2+}, Ni^{3+}, Co^{2+}, and Co^{3+}, which is consistent with the results in literature (Prabu et al., 2014). The N 1s peak (Figure S2) components with binding energies at about 398.68, 399.48, and 400.18 eV are attributable to the quinoid imine (–N=), benzenoid amine (–NH–), and nitrogen cationic ($–N^+–$) of PANI, respectively (Lee et al., 2012).

The Raman spectra of $NiCo_2O_4$ and $NiCo_2O_4$@PANI composites are shown in Figure S3. The peaks at 183.7, 464.4, 513.1, and 659.2 cm^{-1} correspond to E_{2g}, E_g, F_{2g}, and A_{1g} models of $NiCo_2O_4$, respectively (Ma et al, 2015; Shen et al., 2014). Meanwhile, the peaks at 1177 cm^{-1} (C – H bending of benzenoid rings), 1494 cm^{-1} (C = N stretching of the quinoid ring), and 1569 cm^{-1} (C = C stretching of the benzenoid rings) for $NiCo_2O_4$@PANI clearly indicates the presence of PANI (Jeong et al., 2013). In addition, the distinct peak at 1318 cm^{-1} is assigned to the stretching vibration of C–N^+ fragments, indicating the emergence of emeraldine salt of PANI, which is a highly electrical conductive form.

3.2. Electrocatalytic activity toward glucose oxidation.

The dotted lines of the Figure 2 display the cyclic voltammograms (CVs) of different electrodes in 0.1 M NaOH solution. The electrochemical response current of the $NiCo_2O_4$@PANI composite modified GC electrode is much larger than that of the GC electrode and $NiCo_2O_4$ modified electrode, which is attributed to the larger surface area and the super conductivity of $NiCo_2O_4$@PANI nanocomposite. Besides, compared with the GC electrode and $NiCo_2O_4$ modified electrode, the $NiCo_2O_4$@PANI composite modified electrode displays a pair of more distinct redox peaks at 0.35 V and 0.50 V corresponding to the transition of the Ni(II)/Ni(III) redox couple (Singh et al., 1993). Therefore, the $NiCo_2O_4$@PANI composite is considered to enable a more effective electrical contact between redox-active centers and electrolyte, which suggests the potential of $NiCo_2O_4$@PANI nanocomposite modified GC electrode for highly sensitive electrochemical detection. Moreover, the potential of oxidation peak on $NiCo_2O_4$@PANI nanocomposite modified GC electrode is 80 mV negatively shifted compared with that of $NiCo_2O_4$ modified GC electrode. And the peak separation ($\Delta E_p = E_{pa} - E_{pc}$, where E_{pa} and E_{pc} are the anodic and cathodic peak potentials, respectively) for $NiCo_2O_4$@PANI (200 mV) is smaller than that for $NiCo_2O_4$ (340 mV), which indicates that compared with $NiCo_2O_4$ modified GC electrode, the conductivity of the $NiCo_2O_4$@PANI modified GC electrode is relatively improved.

Figure 2 here

The solid lines of the Figure 2 show that the electrocatalytic activity of different electrodes towards the oxidation of glucose (4 mM) in an alkaline medium. The result reveals that the $NiCo_2O_4$@PANI nanocomposite modified GC electrode displays a distinct larger peak current at about 0.5 V than that of GC electrode and $NiCo_2O_4$ modified electrode. The catalytic effect of $NiCo_2O_4$ towards glucose can be described as follows (Zhang et al., 2011):

$$NiCo_2O_4 + OH^- + H_2O - e^- \rightarrow NiOOH + 2CoOOH \quad (1)$$

$$2NiOOH + glucose \rightarrow 2NiO + gluconolactone + H_2O \quad (2)$$

$$NiO + OH^- - e^- \rightarrow NiOOH \quad (3)$$

During the anodic scan, the $NiCo_2O_4$ and NiO species on the electrode surface is converted to NiOOH due to an oxidation reaction [Eq. (1) and Eq. (3)] and in the presence of glucose, the NiOOH species rapidly oxidizes glucose molecules to gluconolactone [Eq. (2)].

Furthermore, the oxidation peak current of $NiCo_2O_4$@PANI nanocomposite modified GC electrode is much higher than that of $NiCo_2O_4$ modified GC electrode. The large enhanced peak current clearly demonstrates that the $NiCo_2O_4$@PANI nanocomposite pose a much higher catalysis towards the oxidation of glucose than $NiCo_2O_4$ nanoparticles. Furthermore, degradation in electrode responses is not observed after repetitive CV scanning, indicating $NiCo_2O_4$@PANI composite electrode is not vulnerable to fouling.

Figure S4 shows the CVs of the $NiCo_2O_4$@PANI composite modified GC electrode recorded at different scan rates (50-250 mV/s). It can be seen that anodic potential shifts more toward the positive potential with the increasing scan rate while the cathodic peak moves negatively. In addition, as is shown in the inset of the Figure S4, the anodic peak currents show linear behavior with the square root of the scan rate, $\upsilon^{1/2}$. The linear regression equation is calculated as I (mA cm^{-2}) = 0.0096 + 1.71 $\upsilon^{1/2}$ (mV/s), revealing the oxidation process of glucose is a surface-controlled electrochemical process (Yu et al., 2011).

These modified electrodes are further used to study their response for the successive injection of glucose to 0.1 M NaOH at 0.50 V and the typical I–T curves are displayed in Figure 3a. As can be seen, the N$NiCo_2O_4$@PANI nanocomposite achieves 95 % of the steady-state current within 5s after the injection of glucose, which indicates a good electrocatalytic performance and a fast electron exchange response of the $NiCo_2O_4$@PANI modified electrode. Furthermore, it is obvious that the steps shown in Figure 3a are more horizontal in the region of a lower concentration of glucose and the noises become higher with the increase in glucose concentration. The noise may be associated with more intermediate species adsorbed onto the electrode due to the increased concentration and prolonged reaction time.

The corresponding current-concentration calibration plots in Figure 3b clearly show that the linear regression equations are Ipa (mA cm^{-2}) = 0.175+4.55C (mM), with R^2=0.9990 for the $NiCo_2O_4$@PANI modified electrode and Ipa (mA cm^{-2}) = 0.349+1.35C (mM), with R^2=0.9776 for $NiCo_2O_4$ modified electrode. At applied

potential of +0.50 V, the sensitivity of the $NiCo_2O_4$@PANI electrode determined by the slope of the linear fitting is 4.55 mA mM^{-1} cm^{-2}, which is obvious higher than that (1.35 mA mM^{-1} cm^{-2}) of the $NiCo_2O_4$ electrode. The high sensitivity is mainly due to the super conductivity and the large active surface area of the $NiCo_2O_4$@PANI composite. Besides, the formation of $NiCo_2O_4$@PANI core–shell network structure provides large amount of highly conductive channels for electron transportation and simultaneously shortening the electron transportation pathway, which leads to fast reaction kinetics increasing the sensitivity of the $NiCo_2O_4$@PANI composite. For the $NiCo_2O_4$@PANI glucose sensor, the linear detection range is from 0.0150 to 4.7350 mM (correlation coefficient =0.9990). The limit of detection (LOD) of the sensor is estimated using the formulae in Equation (4) (Knobel et al, 2012):

$$\mathrm{LOD} = \frac{3s_b}{m} \qquad (4)$$

where s_b is the standard deviation obtained from 10 measurements of the blank signal (5.813×10^{-4} mA cm^{-2}) and m is the slope value of the calibration plot (4.55 mA mM^{-1} cm^{-2}). Therefore, LOD is calculated to be 0.3833 μM. A comparison of the $NiCo_2O_4$@PANI composite with some of the reported non-enzymatic glucose biosensors based on mental oxides or metal hydroxides is summarized in Table 1. From the comparison, the $NiCo_2O_4$@PANI composite exhibits satisfactory performances including high sensitivity, low detection limit and wide linear range. In particular, it has obviously higher sensitivity and lower detection limit than those reported previously. The result above can be attributed to the large surface-to-volume ratio and high conductivity of the $NiCo_2O_4$@PANI nanocomposite, which indicates

that it is a good platform for glucose biosensor.

Figure 3 here

The reproducibility and repeatability of the developed sensor are determined. In a series of 10 sensors prepared in the same way, the relative standard deviation (RSD) of the current response to 4 mM glucose is 3.9 %, indicating the sensor is highly reproducible. The repeatability of one sensor to determine 4 mM glucose is fairly good. The RSD is 2.8 % for 10 successive assays. The response current of this glucose biosensor retains 93.6 % of its initial response current after being stored at 4 °C for two weeks. The avoidance of endogenous interfering species is a big challenge in glucose detection because a few of the structurally similar organic substances (dopamine, uric acid and ascorbic acid) are also simultaneously oxidized along with glucose at the electrode surface and, hence, give interfering electrochemical signals. According to the previous research, the concentration of glucose in human blood is at least 10 times higher than that of the interfering species. The interference experiment of $NiCo_2O_4$@PANI nanocomposite is carried out with successive additions of 1 mM glucose, 0.2 mM dopamine (DA), 0.2 mM ascorbic acid (AA), 0.2 mM uric acid (UA), and 0.2 mM NaCl. Figure S5 indicates that the corresponding change in the oxidation current is about 4.55 mA cm^{-2} upon the addition of 1mM glucose, which far exceeds the changes recorded for the interfering species. Therefore, the $NiCo_2O_4$@PANI nanocomposite presents good selectivity toward glucose detection. The good

selectivity may be attributed to the PANI shell, which prevents the adsorption of poisoning intermediates at $NiCo_2O_4$ surfaces.

4. Conclusions

In summary, the $NiCo_2O_4$@PANI nanocomposite is fabricated via a facile hydrothermal treatment followed by in situ polymerization coating process. The $NiCo_2O_4$@PANI nanocomposite modified electrode displays distinctly enhanced electrocatalytic activity towards the oxidation of glucose. Under the optimal conditions, this constructed glucose biosensor shows more excellent performances such as high sensitivity (4.55 mA mM^{-1} cm^{-2}), low detection limit (0.3833 μM) and wide linear range (0.0150–4.7350 mM). Thus, it is believed that $NiCo_2O_4$@PANI nanocomposite is a promising material in the field of biosensor.

Acknowledgements

This work has been supported by the Programme of Introducing Talents of Discipline to Universities "111" project of China (B08040) and the State Key Laboratory Solidification Processing in NWPU (SKLSP201417).

References

Cao, F., Guo, S., Ma, H. Y., Shan, D. C., Yang, S. X., Gong, J., 2011. Biosens. Bioelectron. 26, 2756-2760.

Ding, Y., Liu, Y.X., Parisi, J., Zhang, L.C., Lei, Y., 2011. Biosensors and

Bioelectronics 28, 393-398.

Ding, Y., Wang, Y., Su, L., Bellagamba, M., Zhang, H., Lei, Y., 2010. Biosensors and Bioelectronics 26, 542-548.

El-Khatib, K.M., Abdel Hameed, R. M., 2011. Biosensors and Bioelectronics 26, 3542-3548.

El-Refaei, S. M., Saleh, M. M., Awad, M. I., 2013. J. Power Sources 223a, 125-128.

Gumpu, M.B., Nesakumar, N., Sethuraman, S., Krishnan, U.M., Rayappan, J. B. B., 2014. Sensors and Actuators B 199, 330-338.

Hu, L. F., Wu, L. M., Liao, M. Y., Hu, X. H., Fang, X. S., 2012. Adv. Funct. Mater. 22, 998-1004.

Jeong, J.M., Choi, B.G., Lee , S.C., Lee , K.G., Chang, S.J., Han, Y.K., Lee, Y.B., Lee, H.U., Kwon, S., Lee, G., Lee, C.S., Huh, Y.S., 2013. Adv. Mater. 25, 6250-6255.

Knobel, G., Calimag-Williams, K., Campiglia, A. D., 2012. Analyst 137, 5639–5647.

Kotanen, C. N., Moussy, F. G., Carrara, S., Guiseppi-Elie, A., 2012. Biosensors Biosensors and Bioelectronics 35, 14-26.

Lee, T., Yun, T., Park, B., Sharma, B., Song, H. K., Kim, B. S., 2012. J. Mater. Chem 22, 21092-21099.

Li, M., Han, C., Zhang, Y. F., Bo, X. J., Guo, L. P., 2015. Analytica Chimica Acta 861, 25-35.

Li, X. C., Sun, W., Wang, L. Q., Qi, Y. D., Guo, T. M., Zhao, X. H., Yan, X. B., 2015. RSC Adv. 5, 7976-7985.

Ma, L.B., Shen, X.P., Zhou, H., Ji, Z.Y., Chen, K.M., Zhu,G.X., 2015. Chemical Engineering Journal 262, 980-988.

Prabu, M., Ketpang, K., Shanmugam, S., 2014. Nanoscale 6, 3173-3181.

Pradhan, D., Niroui, F., Leung, K. T., 2010. ACS Appl. Mater. Interface 8, 2409-2412.

Reitz, E., Jia, W., Gentile, M., Wang, Y., Lei, Y., 2008. Electroanalysis 20, 2482-2486.

Shen, J.F., Li, X.F., Li, N., Ye, M.X., 2014. Electrochimica Acta 141, 126-133.

Singh, N.R., Pandey, P.J., Anitha, L.K., 1993. Int J Hydrogen Energy 18, 467-473.

Sun, S. D., Zhang, X. Z., Sun, Y. X., Yang, S. C., Song, X. P., Yang. Z. M., 2013. ACS Appl. Mater. Interfaces 5, 4429-4437.

Wang, J. P., Thomas, D. F., Chen, A. C., 2008. Anal.Chem. 80, 997-1004.

Wang, L. L., Huang, H., Xiao, S. H., Cai, D. P., Liu, Y., Liu, B., Wang, C. X., Wang, D. D., Li, H., Wang, Y. R., Li, Q. H., Wang, T. H., 2014. ACS Appl. Mater. Interfaces 6, 14131-14140.

Xia, H. S., Wang, Q., 2002. Chem. Mater. 14, 2158-2165.

Xu, W. W., Zhao, K. N., Niu, C. J., Zhang, L., Cai, Z. Y., Han, C. H., He, L., Shen, T., Yan, M. Y., Qu, L. B., Mai. L.Q., 2014. Nano Energy 8, 196-204.

Yang, M., He, J., Hu, X., Yan, C., Cheng, Z., 2011. Environ. Sci. Technol. 45, 6088-6094.

Ye, D. X., Li, H. X., Liang, G. H., Luo, J., Zhang, X. X., Zhang, S., Chen, H., Kong, J.

L., 2013. Electrochimica Acta 109, 195-200.

Yoo, E.H., Lee, S.Y., 2010. Sensors-Basel 10, 4558-4576.

Yu, X. Y., Yao, X. Z., Luo, T., Jia, Y., Liu, J. H., Huang, X. J., 2014. ACS Appl. Mater. Interfaces 6, 3689-3695.

Yu, Z.Y., Li, H.J., Lu, J.H., Zhang, X.M., Liu, N.K., Zhang, X., 2015. Electrochimica Acta 158,264-270.

Zhai, D. Y., Liu, B. R., Shi, Y., Pan, L. J., Wang, Y. Q., Li, W. B., Zhang, R., Yu, G. H., 2013. ACS Nano 7, 3540-3546.

Zhang, Y., Xu, F.G., Sun, Y.J., Shi, Y., Wen, Z.W., Li, Z., 2011. J. Mater.Chem. 21, 16949-16954.

Zhang, Y. Q., Wang, Y. Z., Jia, J. B., Wang, J. G., 2012. Sens. Actuat. B: Chem. 171, 580-587.

Zhang, Y. T., Liu, S. A., Li, Y., Deng, D. M., Si, X. J., Ding, Y. P., He, H. B., Luo, L. Q., Wang, Z. X., 2015. Biosensors and Bioelectronics 66, 308-315.

Zhao, D., Guo, X., Gao, Y., Gao, F., 2012. ACS Appl. Mater. Interface 4, 5583-5589.

Figure captions

Figure 1 (a-c) HRTEM images of $NiCo_2O_4$@PANI nanocomposite. (d) The corresponding EDS spectra.

Figure 2 (a) CV plots of GC electrode, $NiCo_2O_4$ electrode and $NiCo_2O_4$@PANI electrode in the absence (in dotted line) and in the presence (in solid line) of 4 mmol/L glucose in 0.1 mol/L NaOH solution. Scan rate=50 mV/s.

Figure 3 (a) Amperometric response of $NiCo_2O_4$@PANI nanocomposite to successive

additions of glucose at the applied potentials of +0.5 V.

(b) The calibration curve for glucose detection.

Figure 1

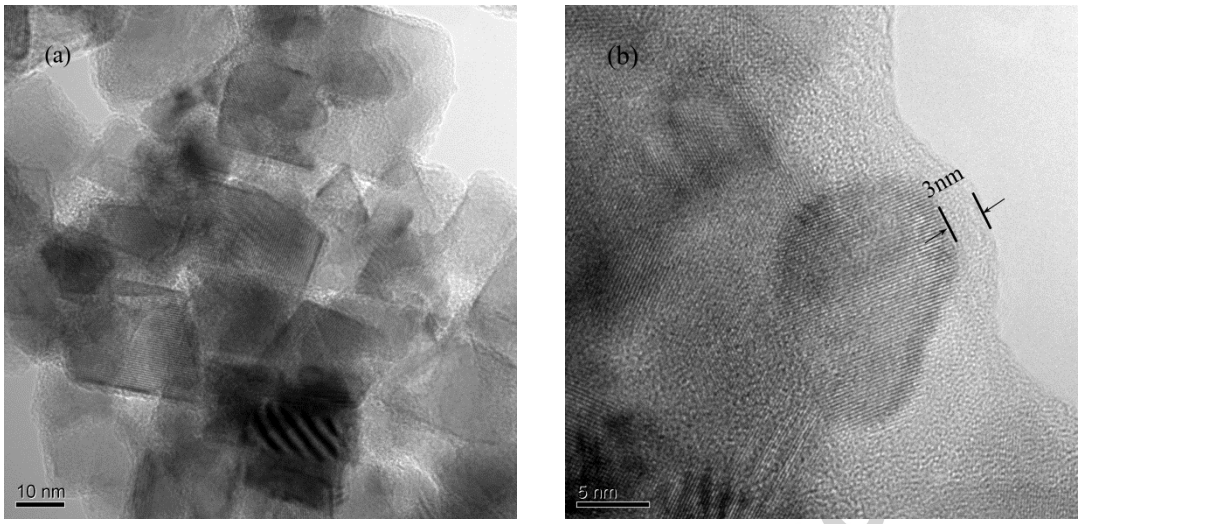

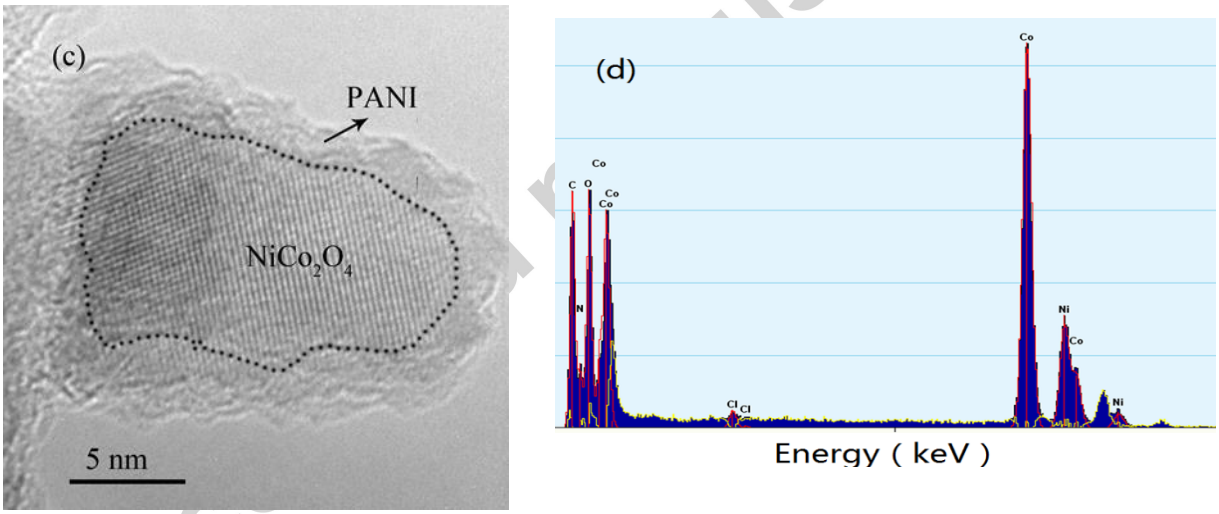

Figure 2

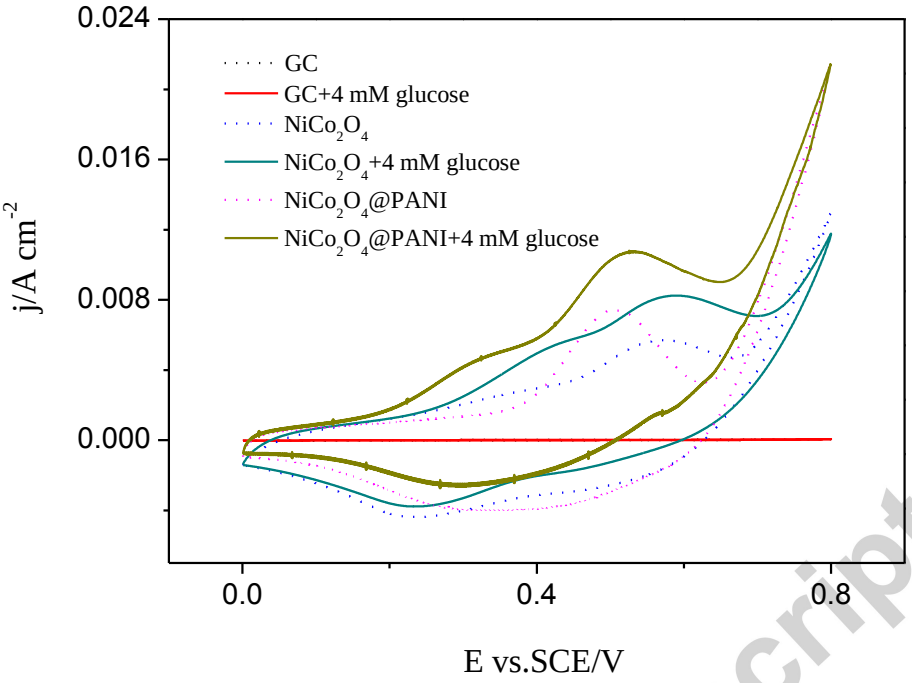

Figure 3

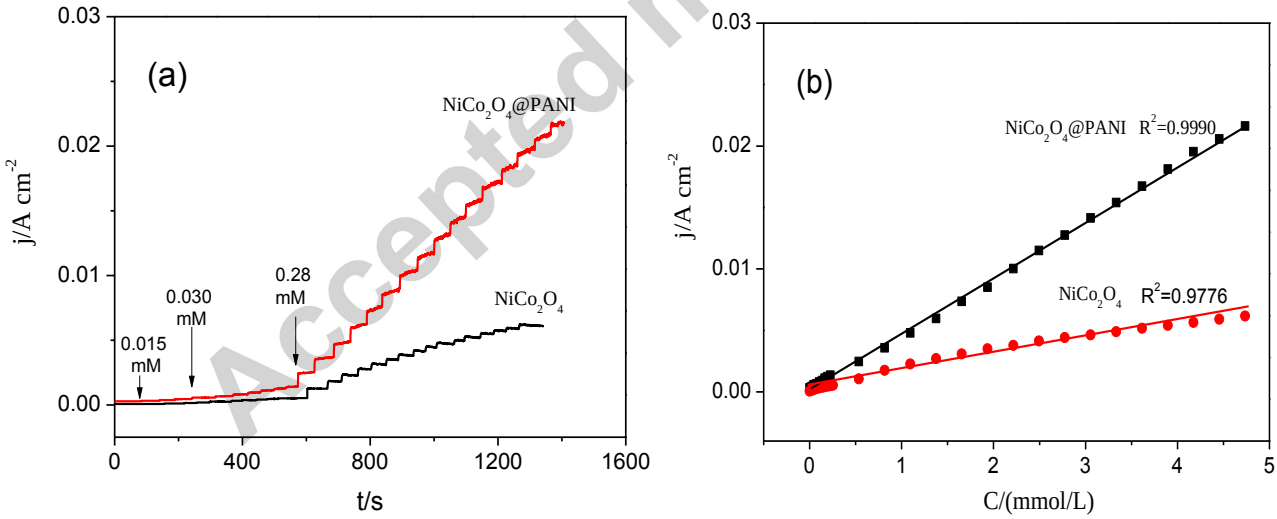

Table 1

Comparison of the performance of $NiCo_2O_4$@PANI composite modified electrode with that of reported non-enzymatic glucose sensors

Electrode material	Sensitivity (μA cm^{-2} mM^{-1})	Linear range (up to, mM)	Detection limit (μm)
GO/NiO nanofibers (Zhang et al., 2012)	1100	0.6	0.77
Co_3O_4 nanofibers (Ding et al., 2010)	36.25	2.04	0.97
NiO–Au hybrid nanobelts (Ding et al., 2011)	48.35	4	0.65
Cu_2O/Carbon Vulcan XC-72 (El-Khatib and Abdel-Hameed, 2011)	232	3	2.6
CuO nanosphere (Reitz et al., 2008)	404.5	2.55	1
This work	4550	4.7350	0.3833

Highlights：

1. The core-shell structure of $NiCo_2O_4$@Polyaniline nanocomposite is fabricated via a facile hydrothermal treatment followed by in situ polymerization coating process.

2. The average diameter of these $NiCo_2O_4$@Polyaniline nanoparticles is only about 25 nm which greatly shortens the ion-transport pathways.

3. Owing to the outstanding conductivity of Polyaniline shell, the $NiCo_2O_4$@Polyaniline core-shell structure can realize fast reaction kinetics leading to high sensitivity for the determination of glucose.

4. Due to the good protection of Polyaniline shell, the core-shell composite shows excellent electrochemical stability.